eISSN 2005-5447
International Journal of Stem Cells Vol. 16, No. 1, 2023 https://doi.org/10.15283/ijsc21238

ORIGINAL ARTICLE

Synergistic Effect of Hydrogen and 5-Aza on Myogenic Differentiation through the p38 MAPK Signaling Pathway in Adipose-Derived Mesenchymal Stem Cells

Wenyong Fei[1,*], Erkai Pang[2,*], Lei Hou[2], Jihang Dai[1], Mingsheng Liu[2], Xuanqi Wang[2], Bin Xie[2], Jingcheng Wang[1]

[1]*Department of Sports Medicine, Northern Jiangsu People's Hospital, Clinical Medical College, Yangzhou University, Yangzhou, China*
[2]*Department of Sports Medicine, Northern Jiangsu People's Hospital, Dalian Medical University, Dalian, China*

Background and Objectives: This study aims to clarify the systems underlying regulation and regulatory roles of hydrogen combined with 5-Aza in the myogenic differentiation of adipose mesenchymal stem cells (ADSCs).
Methods and Results: In this study, ADSCs acted as an *in vitro* myogenic differentiating mode. First, the Alamar blue Staining and mitochondrial tracer technique were used to verify whether hydrogen combined with 5-Aza could promote cell proliferation. In addition, this study assessed myogenic differentiating markers (e.g., Myogenin, Mhc and Myod protein expressions) based on the Western blotting assay, analysis on cellular morphological characteristics (e.g., Myotube number, length, diameter and maturation index), RT-PCR (Myod, Myogenin and Mhc mRNA expression) and Immunofluorescence analysis (Desmin, Myosin and β-actin protein expression). Finally, to verify the mechanism of myogenic differentiation of hydrogen-bound 5-Aza, we performed bioinformatics analysis and Western blot to detect the expression of p-P38 protein. Hydrogen combined with 5-Aza significantly enhanced the proliferation and myogenic differentiation of ADSCs *in vitro* by increasing the number of single-cell mitochondria and upregulating the expression of myogenic biomarkers such as Myod, Mhc and myotube formation. The expressions of p-P38 was up-regulated by hydrogen combined with 5-Aza. The differentiating ability was suppressed when the cells were cultivated in combination with SB203580 (p38 MAPK signal pathway inhibitor).
Conclusions: Hydrogen alleviates the cytotoxicity of 5-Aza and synergistically promotes the myogenic differentiation capacity of adipose stem cells via the p38 MAPK pathway. Thus, the mentioned results present insights into myogenic differentiation and are likely to generate one potential alternative strategy for skeletal muscle related diseases.

Keywords: Hydrogen, 5-Azacitidin (5-Aza), Myogenic differentiation, Adipose-derived mesenchymal stem cells, P38 MAPK signaling pathway

Received: December 10, 2021, Revised: May 18, 2022, Accepted: June 13, 2022, Published online: August 31, 2022
Correspondence to **Jingcheng Wang**
Department of Sports Medicine, Northern Jiangsu People's Hospital, Clinical Medical College, Yangzhou University, 98# Nantong xi Road, Yangzhou 225001, China
Tel: +86-13909254888, Fax: +86-051487373425, E-mail: sbydyxwjc@163.com
*These authors contributed equally to this work.

Introduction

Skeletal muscle is commonly impaired for various causes (e.g., trauma and sports activities). The tissue exhibits self-regenerating capability and the inherent satellite cell activity, activating, differentiating and fusing to other satellite cells for forming myotubes with multinucleation (1). Myotubes have the integration of the existed fibers for the regeneration. Nevertheless, volumetric muscle loss (VML), especially due to tumor removal, degeneration or high-energy trauma, cannot complete the mentioned cascade since fibrosis has more rapid propagation as compared with myogenesis (2, 3). There is no feasible treatment option for muscle degeneration process and muscle volume loss. Therefore, there is an urgent need for a novel treatment method with few complications and satisfactory results.

In recent years, researchers have attempted to use biological and regenerative medicine approaches to promote myogenic differentiation to meet the criteria for biological healing. Stem cells are of great interest in tissue engineering and regeneration due to their excellent regenerative potential, immunomodulation and heritability (4, 5). Based on the above advantages, stem cells are highly expected to promote myogenic differentiation. ADSCs are a fairly efficient source of adult multipotential stem cells and are readily available (6). In addition, existing study reported (7) differentiating ability exhibited by ADSCs to various lineages including bone (8), cartilage (9), muscle (10) and nerve (11). Besides, as suggested by Mizuno et al. (12), ADSCs could achieve myogenic differentiation. However, studies have shown that only 15% of the stem cells harvested from processed adipose aspirates can be fully differentiated. In contrast, direct transplantation of stem cells into target organs has obvious drawbacks such as difficulty in homing to the site of injury, low cell viability, and inefficiency in local differentiation (13). Thus, the clinical myogenic differentiation potential of ADSCs is limited. At present, researchers try to promote myogenic differentiation of stem cells in different ways, such as drug induction, physical induction, cell scaffold induction and so on. Among them, drugs as a more mainstream way of induction, but there are some problems, such as low induction efficiency, obvious inhibition of stem cell self-renewal ability and so on (4). Therefore, how to obtain an efficient rate of myogenic differentiation of stem cells in the repair area is the main challenge in the treatment of muscle injury.

5-Azacitidine (5-Aza) is a DNA methylation inhibitor similar to cytidine and is known to promote the upregulation of muscle genes and myogenic differentiation. At present, 5-Aza is the most commonly used chemical agent to induce the myogenic differentiation of stem cells. However, according to some reports, 5-Aza has carcinogenic and toxic effects on cells. Therefore, the ability to enable ADSCs to obtain efficient myogenic differentiation without reducing cell activity is a major challenge in the treatment of muscle injury.

Hydrogen (H_2), one kind of endogenous gas, was suggested to be one vital energy origin and to critically impact physiologically-related regulating process (14). Hydrogen molecules can enter tissue as well as performing anti-inflammation-related, antioxidant and anti-apoptotic effects (15). It is noteworthy that H_2 exhibits great efficacy and safety to cases clinically (16). For example, Aoki et al found that hydrogen reduced the blood lactic acid level of male football players (17) and improved the decline of muscle function caused by exercise. H_2 can also reduce exercise-induced muscle injury and delayed muscle atrophy, but has no effect on peripheral neutrophil count and neutrophil dynamics and function (18). In the mouse hindlimb Istroke R injury model, H_2 inhalation significantly reduced the infarct area and tissue structure loss area, alleviated muscle injury, and enhanced functional recovery (19). Then, whether hydrogen can alleviate the cytotoxicity of 5-Aza and thus enhance myogenic differentiation of stem cells still needs further investigation.

As indicated from the existing research, ERK1/2, NF-kB, Notch and Wnt signal pathways are capable of regulating the forming and reconstructing processes of general skeletal muscle (20-23). Moreover, the p38 MAPK class refers to the signal transducing elements that can facilitate the muscle differentiation *in vitro*, impact the *in vivo* growth and repair of skeletal muscle, and directly affect the myogenic transcribing elements pertaining to the Myod family (24, 25). The p38 MAPK not only functions as a muscle-specific gene switch, but is also a regulator of muscle damage and a key factor in maintaining muscle homeostasis (26). Therefore, whether H_2 combined with 5-Aza regulates the biological effects of adipose stem cells through the p38 MAPK signaling pathway remains to be further demonstrated.

The hypothesis of this study is that H_2 combined with 5-Aza enhances myogenic differentiation of adipose mesenchymal stem cells via the p38 MAPK signaling pathway. To test this hypothesis, we evaluated the effect of hydrogen combined with 5-Aza on adipose stem cell myogenic differentiation and its molecular mechanism by molecular biology and reverse transcription polymerase.

Materials and Methods

Materials

Five healthy 2-week-old male rats (Animal Experiment Center of Yangzhou University, Yangzhou, China), adipose stem cells (isolated from primary cells), DMEM medium (Hyclone, USA), 10% Fetal bovine serum (FBS) (Hyclone, USA), H_2 incubator includes hydrogen concentration (70%), oxygen concentration (21%), carbon dioxide concentration (5%) and nitrogen concentration (4%) (Wuxi Puhe Bio-pharmaceutical Technology Co., A001, Wuxi, China), 10 μmol/l 5-azacytidine (5-Aza) (27), 5 uM SB203580 (Beyotime S1863, Shanghai, China), 3-(4,5-dimethylthiazol)-2,5-diphenyl-tetrazolium bromide (MTT) (Sigma, USA), Dimethyl sulfoxide (DMSO) (Invitrogen, USA), Alamar blue kit (Beijing solarbio science and technology co.,ltd., A7631, Beijing, China), Live-Dead Cell Staining Kit (Biovision, K501-100, USA), Mito-tracker (Beyotime, C1048, Beijing, China), Reverse transcription reagent tool (Thermo, K1622, Shanghai, China), SYBRGreen PCR kit (Thermo, F-415XL, Shanghai, China), BCA protein assay kit (KGPBCA, Nanjing, China), Alizarin red staining kit (Solarbio, G8550, Beijing, China), Toluidine blue staining kit (Solarbio, G3661, Beijing, China), Oil red O staining kit (Solarbio, G1262, Beijing, China), β-actin antibody (Proteintech, 60008-1-lg, USA), Myosin antibody (Proteintech, 60229-I-Ig, USA), Desmin antibody (Proteintech, 16520-1-AP, USA), Myod (Proteintech, USA), Mhc (Bioss, bs-10904R, Beijing, China), p-P38 (Affinity, USA), GAPDH (Proteintech, USA), Anti-rabbit secondary antibody labeled by CY3 (Proteintech, SA00009-2, USA), Anti-mouse secondary antibody labeled by CY3 (Proteintech, SA00009-1, USA), Hoechst (Beyotime, Beijing, China), CD45 antibody (BD Biosciences, 555485, USA), CD44 antibody (BioLegend, 103011, USA), CD90 antibody (BD Biosciences, 555595, USA), CD31 antibody (Abcam, ab64543, USA).

Methods

Extraction and cultivation of ADSCs: All animal experiments were performed under the approval of the Institutional Animal Care and Use Committee of Yangzhou University (Approval No. DWLL-202112-201). Five two weeks old male SD rats were euthanized with excessive ether asphyxiation. The rats were routinely disinfected by 75% ethyl alcohol, and their blood vessels, fascia and other tissues were removed. The harvested inguinal adipose tissue was cut into 1 mm^3 pieces and then placed into a 15 ml centrifuge tube. 0.1% type I collagenase was used to digest tissue for 40～60 min. After filter to remove nondigested tissue, filtrate was collected and seed into tissue culture plastic in culture medium with 10% fetal bovine serum. The incubation was conducted at 37℃ with a volume fraction of 5% CO_2, and the liquid was altered after 24 h, 48 h and 72 h. Under the cell concentration of 80%, 0.25% trypsin-EDTA was employed for digestion and subculture. The 3rd generation cells were employed for the immunocytochemical identification and subsequent tests.

Bioinformatics analysis: Data retrieved was performed in the GEO database by search the key words “Hydrogen”. And finally GSE62434 was obtained to analyze the expression of fibroblasts cultured in hydrogen. Fibroblasts were divided into groups according to whether they were cultured or not. The differentially expressed genes were obtained by GEO2R online tool. KEGG enrichment analysis was performed based on the differentially expressed genes in the DAVID online website. GSEA enrichment analysis of differentially expressed genes was subsequently performed using GSEA software.

Identification of ADSCs: ADSCs were cultured and then identified when 90% of the cells were covered. The cells were digested by trypsin at ambient temperature for 10 min, and it was collected after being centrifuged. Subsequently, the cells were washed with PBS and then prepared into 1×10^5/ml cell number suspension. 100 μl of 1×10^5 cell suspension was added with 10 μl of fluorescently labeled phenotypic antibody (CD45, CD44, CD90 and CD31) respectively for incubation. After the washing process, the expressions of CD45, CD44, CD90 and CD31 surface antigens were detected by performing the flow cytometry.

Identifying process for three-line differentiation of ADSCs: The multilineage differentiating potentials of ADSCs were characterized by osteogenic, adipogenic, and chondrogenic differentiation. Briefly, according to 5×10^4 cells/cm^2 cell density, cells received the collecting and inoculating processes inside the orifice plate. The cells received the culturing process with 5% CO_2 at 37℃. Under the cell confluence of 90%, The cells were cultured in osteogenic, adipogenic and chondrogenic differentiation media and identified and analyzed by alizarin red (Solarbio, G8550, Beijing, China), oil red O (Solarbio, G1262, Beijing, China), toluidine blue staining (Solarbio, G3661, Beijing, China). Stained areas were observed under a fluorescence microscope (OLYMPUS, IX71).

Groups and cell proliferation of ADSCs: The cells were seeded in 96-well plates (Thermo Scientific, USA) at 1×10^4/well in 100 μl of DMEM with FBS. The groups (control, H_2, 5-Aza and H_2+5-Aza) were tested at days 1,

2 and 3. Furthermore, the control and 5-Aza groups were incubated in a conventional cell incubator (5% CO_2, 95% air) and the H_2 and H_2+5-Aza groups were incubated in a hydrogen incubator (70% hydrogen, 21% oxygen, 5% CO_2, 4% nitrogen). The cell proliferation ability of H_2 and 5-Aza was compared by MTT and Alamar blue staining respectively. Cells were stained with MTT (20 μl; 5 mg/ml) for 4 h at 37℃. Dimethyl sulfoxide was added to samples and incubated for 30 min at 37℃. The absorbance was measured using a microplate reader (Thermo MK3 type) at 492 nM.

Cell samples were taken, and 10 μl Alamar blue staining was introduced to 100 μl cell suspension at 1- and 3-day induction time. Incubating in an incubator away from light for 6 h, and detecting with microplate reader with a wavelength of 600 nm. The diluted AM/PI kit (Biovision, K501-100, USA) was added and incubated for 30 min before washing. Observed by means of fluorescence microscope (OLYMPUS, IX71). Red and green denote dead cells and live cells, respectively. With ImageJ software (National Institutes of Health, Bethesda), this study determined the fluorescence intensity.

Effect of hydrogen on mitochondria by mito-tracker green fluorescent staining: To investigating the influence exerted by H_2 for mitochondria. First, ADSCs received the inoculating process on confocal petri dishes and the culturing process inside normal medium for 12 h. Next, the cells received the seven-day incubation with control, H_2, 5-Aza, H_2+5-Aza. Then, the medium received the removal and rinsing process by applying PBS, and then it was incubated with the mito-tracker (1 : 5,000～1 : 50,000) at 37℃ for 15～45 min. Lastly, under a Laster confocal fluorescence microscope, the observation of cells was conducted.

Immunofluorescence detecting process of the expressions of Desmin, Myosin and β-actin in cells: After incubation with control, H_2, 5-Aza, H_2+5-Aza for 7 days, ADSCs were fixed in 4% paraformaldehyde for 15 min. Then, 0.1% Triton was used for stabilization at ambient temperature for 15 min. The cells were sealed with 5% FBS for 15 min under the temperature of the ambient. Subsequently, the cells were incubated by using primary antibody at 4℃ throughout the night. After washing, it was incubated at 37℃ for 1 h by using secondary antibody. Hochest received the incubating process under ambient temperature and the isolating process away from light for 15 min. Lastly, with the use of a fluorescence microscope (OLYMPUS, IX71), the samples were observed.

Real-time PCR analysis of Myod, Mhc and Myogenin: Under the p38 MAPK signal pathway inhibitor (SB203580), the cells were collected after being inducted with control, H_2, 5-Aza, H_2+5-Aza for 7 days. Overall RNA was extracted from the cells under the transfection with the Trizol extraction tool in accordance with the guidelines of the producer. According to the guidelines of the producer, cDNA received the synthesis based on reversely transcribing process with the first strand cDNA synthesis tool. Primers for reverse transcription PCR received the designing and synthesizing processes with Primer Premier 5.0 software (Shanghai Biotechnology, China) based on internal reference of housekeeper gene GAPDH. After PCR amplification, the results were automatically analyzed by using the fluorescence quantitative PCR tool in the real time, the baseline and threshold were regulated in accordance with the negative control to determine the Ct value of the respective specimen, as well as whether the Ct value was effective based on the fusion curve. For the export, the $2^{-\Delta\Delta Ct}$ approach inside gene expressing state differences of control and the concentration groups is: ΔCt=Ct gene −Ct inside. Subsequently the control group ΔCt remember was obtained for ΔCt contrast, ΔCt contrast average was achieved, in which the respective group of ΔCt minus ΔCt contrast average, calculated by $\Delta\Delta$Ct value, i.e., the $\Delta\Delta$Ct=ΔCt sample-ΔCt contrast, next, the respective group $2^{-\Delta\Delta Ct}$ value was calculated, which indicated the comparative expressions of genes.

Observation and analysis of myotube: To investigate the effect of H_2 combined with 5-Aza on the myogenic differentiation system of ADSCs, the authors introduced the SB203580 (5 uM) to the culture medium (DMEM). Under the p38 MAPK signal pathway inhibitor (SB203580), cells were collected after being inducted with control, H_2, 5-Aza, H_2+5-Aza for 7 days. First, ADSCs received the inoculating process on 24-well plates under a density of 8000 cells/cm for 12 h. Subsequently, the cells were further cultured at a concentration of 70% H_2, and the medium received the renewal every two days. Myotube formation in ADSCs regulated by H_2 combined with 5-Aza was measured by immunofluorescence staining. ImageJ software was used to obtain the index maturation of myotube (National Institutes of Health, Bethesda, USA).

Western blotting assay: ADSCs were placed in 3.5 cm culture dishes with or without SB203580 and cultured with control, H_2, 5-Aza and H_2+5-Aza for 7 days. Next, cell mass was washed three times with PBS, lysed for 30 min in ice-cold RIPA lysis buffer, and then its protein was quantified. According to the number of samples, the authors introduced the 200 μl BCA working solution (KGPBCA) in samples, and determined the absorbance at 562 nm. After being denaturalized, the protein was admin-

istrated with polyacrylamide gel and then transferred to the methanol-activated PVDF membrane. After being blocked, the primary antibody was incubated at 4℃ throughout the night: Myod (Proteintech, 1 : 1,000～1 : 6,000), Mhc (Bioss, bs-10904R, 1 : 500), p-P38 (Affinity, 1 : 500～1 : 2,000), GAPDH (Proteintech, 1 : 5,000). The PVDF membrane was introduced into rabbit secondary antibody or rat secondary antibody (ZSGB-BIO, 1 : 5,000) solution under the dilution with 1 : 5,000 HRP-labeled solution and was incubated at 37℃ under L h slow oscillation. By employing ECL luminescent solution (Beijing Dingguo ECL-0011), the imprints were developed, and by adopting Image J (NIH, Bethesda, USA), the immunoreaction bands received the quantification.

Statistical analyses

All experiments were performed in triplicate. For the data recording and the statistical analyses, SPSS 24.0 software in terms of Windows (SPSS Inc., Chicago, IL, USA) was used. The information has the expression to be the mean±standard deviation (SD) pertaining to a range of measuring processes. The authors performed student's t testing process for comparing one individual experiment-related mean with the control mean. $p<0.05$ exhibited statistical significance.

Results

Bioinformatics analysis results

According the GEO2R online tool, a total of 576 differentially expressed genes was obtained, of which 267 were upregulated differentially expressed genes and 199 were downregulated differentially expressed genes (Fig. 1A and 1B). KEGG enrichment analysis and GSEA enrichment analysis of the differentially expressed genes showed that the differentially expressed genes were mainly enriched in p38, MAPK signaling pathway, mitochondria related pathways (Fig. 1C～F).

The evaluation of ADSCs

ADSCs were identified by flow cytometry: ADSCs have no specific surface antigens. Accordingly, the analysis of multiple surface antigens simultaneously to determine the characteristics of adipose stem cells. By flow cytometry, the ADSCs surface markers was tested. We examined the expression of CD31, CD44, CD45 and CD90 in ADSCs. Flow cytometry results showed that 1.6% expressed CD31, 95.2% expressed CD44, 1.1% expressed CD45, and 97.4% expressed CD90 (Fig. 1G). CD44 (95.2%) and CD90 (97.4%) express stem cells. The low expressions of CD31 (1.6%) and CD45 (1.1%) excluded epidermal cells and vascular endothelial cells, respectively. This characteristic meet the criteria stated by the International Society for Cellular Therapy (ISCT) for MSC.

ADSCs were identified by three-line differentiation: The multilineage differentiating potentials of ADSCs were characterized through the osteogenic, adipogenic and chondrogenic differentiation. Alizarin red staining under the induction by ADSCs osteogenesis are presented in Fig. 1H (a), demonstrating the appearance of considerable osteoblasts when the induction was achieved. Fig. 1H (b) shows the staining process of oil red O when the adipogenic induction was achieved, and the stained cells were observed as well. Fig. 1H (c) shows the staining of toluidine blue when the chondroblast induction was achieved, and many chondrocytes were stained. In brief, the mentioned cell could achieve a three-line differentiation, which demonstrated that it acts as a rat ADSCs.

Biocompatibility evaluation of hydrogen

The optimal concentration of hydrogen: Whether H_2 could promote cell viability and proliferation was evaluated by MTT assay (Fig. 2F). After being cultured with H_2 at different concentrations (20%, 50%, 70%), ADSCs showed different cell viability and proliferation. On day 1, no significant difference was fund between the four groups (Control, 20%H_2, 50%H_2, 70%H_2) ($p>0.05$). As compared with other three groups, cells displayed a remarkably high proliferation in 70%H_2 group ($p<0.01$) on day 2 and 3. Subsequent experiments were performed at 70% concentration of H_2.

Assessment of cell proliferation by hydrogen: First, we evaluated whether H_2 could promote cell viability and proliferation by MTT and Alamar blue Staining (Fig. 2A～E). In H_2 group, when cultivated for 1 and 3 days, the cells were primarily alive (green), while few had death (red) (Fig. 2A and 2C). In addition, the cell proliferation characteristic received the quantitative analysis of Live-Dead Cell Staining. As compared with the 5-Aza group, cells displayed a remarkably high proliferation in H_2 group ($p<0.01$) on day 1. There was no significant difference between the other three groups (Control, H_2, 5-Aza+H_2) ($p>0.05$). On day 3, compared with 5-Aza and 5-Aza+H_2 groups, H_2 group displayed the highest expression ($p<0.01$). Compared with the 5-Aza group, the survival rate of cells in the 5-Aza+H_2 group was still higher ($p<0.01$).

Furthermore, the cell proliferation behavior was quantitatively analyzed by Alamar blue assay. On day 1, the cell viability in H_2 group was significantly higher than other

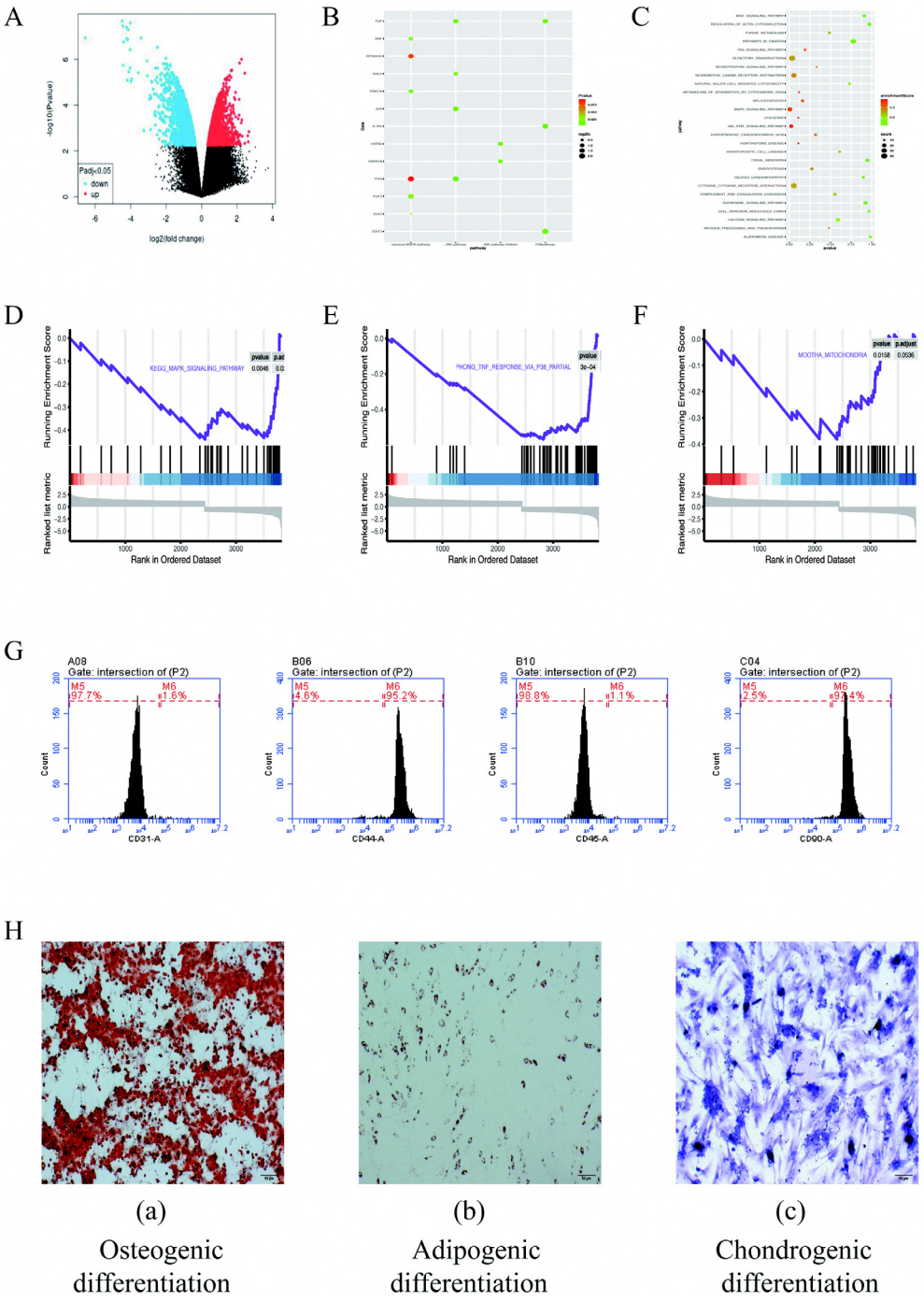

Fig. 1. (A) Volcanic map of cells cultured in hydrogen shows differentially expressed genes. (B) KEGG enrichment pathway analysis. (C) Analysis of differential gene expression in MAPK signaling pathway, GSEA enrichment analysis. (D) Enrichment analysis of MAPK signal pathway. (E) Enrichment analysis of p38-MAPK signal pathway. (F) Mitochondrial functional enrichment analysis. (G, H) Identifiification of adipose-derived stem cells (ADSCs). (G) Flow cytometry analysis results and expression of cell surface CD markers of ADSCs at passage 3. The x-axis is the fluorescence intensity, and the y-axis is the cell number (H). ADSCs was positive for Alizarin red (a), Oil Red O (b), and Toluidine blue staining (c) after induced differentiation.

groups (5-Aza, 5-Aza+H_2) ($p<0.01$). And, compared with the control group, only the H_2 group showed high proliferation ($p<0.05$). Interestingly, compared with the 5-Aza group, the 5-Aza+H_2 group also showed significantly higher proliferation ($p<0.01$). On day 3, the cell viability in H_2, 5-Aza and 5-Aza+H_2 groups maintained

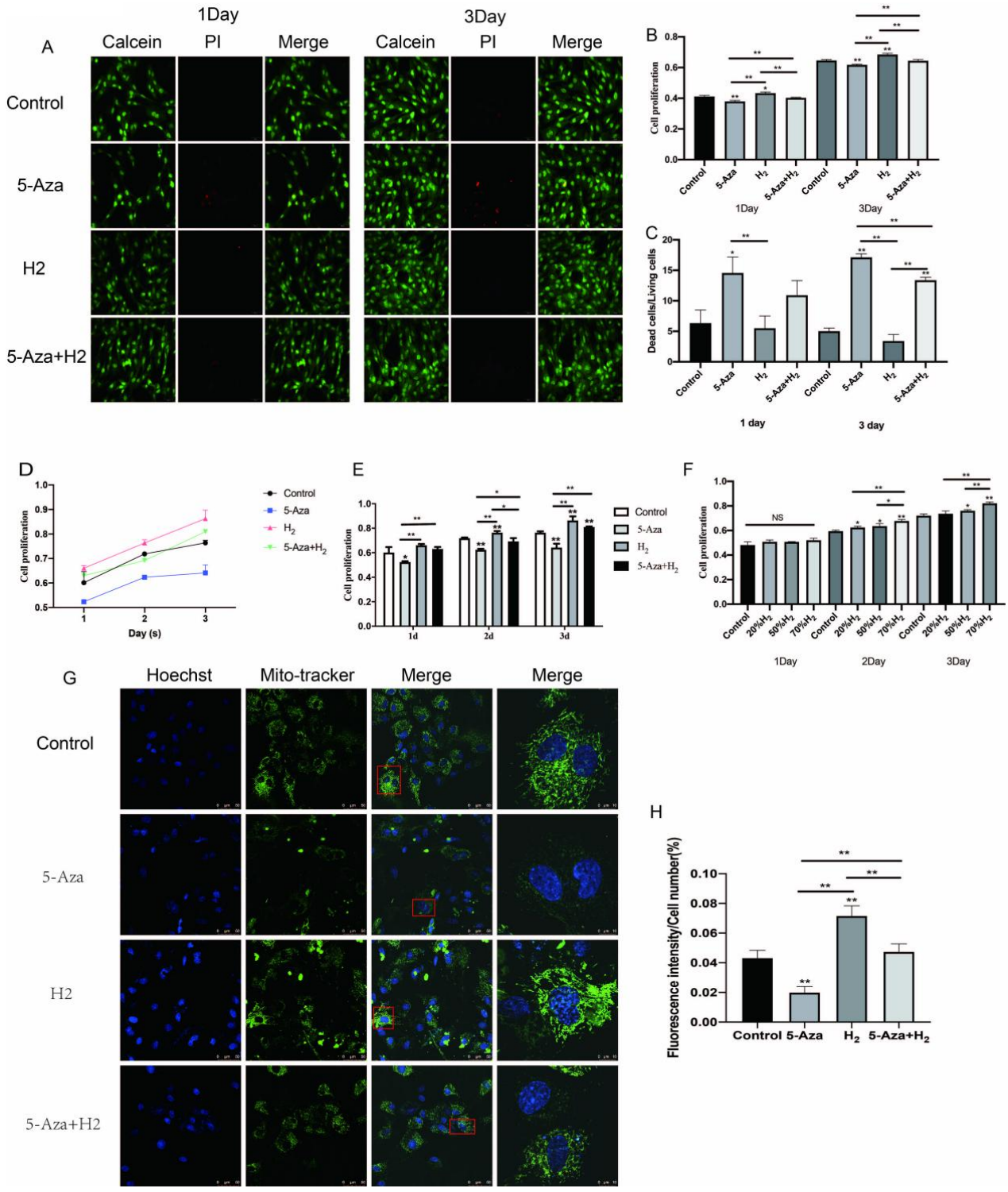

Fig. 2. (A～C) ADSCs viability evaluation after cultured with different differentiation medium for 1 to 3 days. (A) Live-Dead cell staining analysis and Alamar blue staining on 1 and 3 days. (B) Fluorescence quantitative analysis of cell proliferation. (C) Proportion analysis of Live-Dead cells. (D, E) Cell viability was assessed by MTT. (F) Selection of the optimum concentration of hydrogen. (G, H) The analysis of mitochondrial staining. (G) Fluorescent staining of mitochondria by Mito-tracker. (H) Quantitative analysis of fluorescence intensity of single cell mitochondria. All experiments were performed in triplicate (*$p<0.05$, **$p<0.01$).

the same trend as day 1 (Fig. 2B). Based on MTT analysis (Fig. 2D and 2E), compared with the 5-Aza group, the H_2 group significantly promoted cell proliferation in the first three days ($p<0.01$). At the same time, compared to the 5-Aza group, the 5-Aza+H_2 group also increased cell proliferation ($p<0.05$). As demonstrated by all the mentioned results, H_2 remarkably enhanced the ADSCs proliferation.

Mito-tracker green fluorescent staining: The green mito-tracker staining was performed for explaining the effect of H_2 on the mitochondria function of ADSCs (Fig. 2G and 2H). Obviously, compared with the other three groups, H_2 group expressed significant single-cell mitochondrial fluorescence intensity ($p<0.01$). Compared with the control group, the intensity of green fluorescence was significantly decreased in the 5-Aza group ($p<0.01$), and the fluorescence expression of single-cell mitochondria was also significantly increased in the 5-Aza+H_2 group compared with the 5-Aza group ($p<0.01$).

Myogenic differentiating effect of hydrogen

Immunofluorescence detecting process of the expressions of Desmin, Myosin and β-actin in cells: To investigate the effect of H_2 combined with 5-Aza on myogenic differentiation at the myoblast stage, ADSCs were employed as an *in vitro* model of myogenic differentiation. The cells were respectively cultured with 5-Aza, H_2, H_2+5-Aza for 7 days. Fig. 3A shows the results of immunofluorescence staining assay after incubation for 7 days. The immunofluorescence results showed that remarkably higher immunofluorescence expressing states of β-actin and desmin in the H_2 group and 5-Aza group than in the control ($p<0.01$). In addition, compared with the control group, the H_2 group showed increased myosin expression ($p<0.05$). Additionally, the expressing states of all test antibody were remarkably higher in the H_2+5-Aza group than in the H_2 group ($p<0.01$). It is noteworthy that the expressing states of the β-actin in 5-Aza and H_2 group were found, whereas noticeable difference was identified between the two groups ($p<0.01$). Additionally, the expressing states of Mhc antibody were remarkably higher in the H_2+5-Aza group than in the other group (5-Aza and H_2 groups) ($p<0.05$).

Observation and analysis of myotube: Mhc protein immunofluorescence staining assay was studied to observe the morphology of myotubes formed in ADSCs. Fig. 3B shows the results of immunofluorescence staining assay after 7 days of incubation. The number, length, diameter and maturation index of myotubes were quantified by morphological analysis. Myotube maturation was quantified by measuring the ratio of the number of cells with more than 2 nuclei to the total number of cells (maturation index). The remaining three groups (5-Aza, H_2 and 5-Aza+H_2) showed statistically significant differences in myotube number, length, diameter and maturation index compared to Control ($p<0.01$). Notably, the 5-Aza+H_2 group exhibited the best myotube number, length, diameter and maturation index compared to the 5-Aza and H_2 groups ($p<0.05$) (Fig. 3B a~d). After the introduction of the p38 MAPK signaling pathway inhibitor (SB203580), the number, length, diameter and maturation index of myotubes were lower in the 5-Aza, H_2 and 5-Aza+H_2 groups (Fig. 3B e~h).

Real-time PCR analysis of Myod, Mhc and Myogenin: We further investigated the effect of the H_2 combined with 5-Aza on myogenic genes expression of ADSCs *in vitro*. Myod, Myogenin and Mhc, the early and late markers of myogenesis, were used to determine the myogenic differentiation at mRNA level (Fig. 3C). After being cultured for 7 days, the quantitative RT-PCR results showed remarkably higher mRNA expressing states of MyoD, Myogenin and Mhc in the H_2+5-Aza+SB203580 group than other four group ($p<0.01$). However, compared with the SB203580 group, the expression of MyoD, Myogenin and Mhc genes was significantly higher in the H_2 group ($p<0.01$). No noticeable difference was identified in MyoD, Myogenin and Mhc RNA expressions among the H_2+SB203580 and 5-Aza+SB203580 groups ($p>0.05$). As impacted by SB203580, the expressions of MyoD, Myogenin and Mhc of the inhibitor groups was also a little less than control group ($p<0.05$).

Western blotting assay of Myod, Mhc and Myogenin: In addition, under the expressing states of Myogenin and Myod (early myogenic marker) and the differentiated myotube marker myosin heavy chain (Mhc), we conducted the western blotting assay for assessing myogenic differentiation (Fig. 4A b~d). As revealed from the results of the western blotting assay, remarkably higher stripe expressing states of Myod, Mhc and Myogenin were found in the H_2 group, 5-Aza group and 5-Aza+H_2 group as compared with those in the control ($p<0.01$). The protein expression status of Myod, Myogenin and Mhc was significantly higher in the H_2+5-Aza group than in the H_2 and 5-Aza groups ($p<0.01$).

Effect of hydrogen combined with 5-Aza on the phosphorylation of p38 in myogenic differentiation

According to the mentioned results, H_2 combined with 5-Aza significantly improves the proliferation and myogenic differentiation of ADSCs, whereas the molecular system was unclear. Through the analysis of bioinfor-

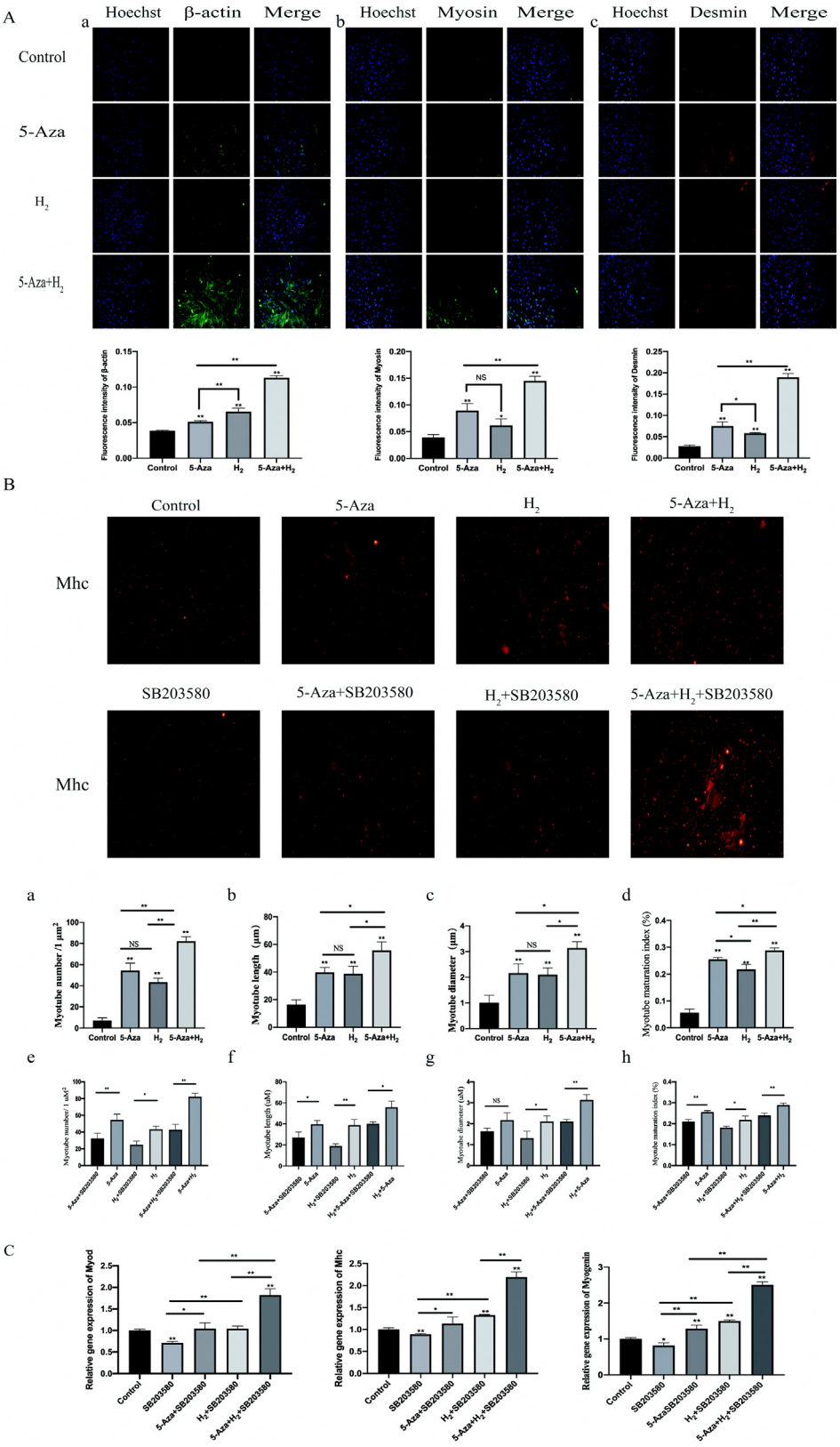

Fig. 3. (A) β-actin, Myosin and Desmin expression (Immunofluorescence staining). Molecular expression levels of (a) β-actin, (b) Myosin and (c) Desmin. (B) Observation and analysis of myotube. Immunofluorescence staining of Mhc protein (red) in ADSCs on day 7 in myogenic differentiation medium; Quantitative analysis of Myotube number (a), Myotube length (b), Myotube diameter (c), Myotube maturation index (myotubes with≥2nuclei) (d), Comparison of the number of myotubes between the groups (e), Comparison of myotube length between groups (f), Comparison of myotube diameter between groups (g), and comparison of myotube maturation index between groups (h). (C) Myod, Mhc and Myogenin expression (RT-PCR). All experiments were performed in triplicate (*$p<0.05$, **$p<0.01$).

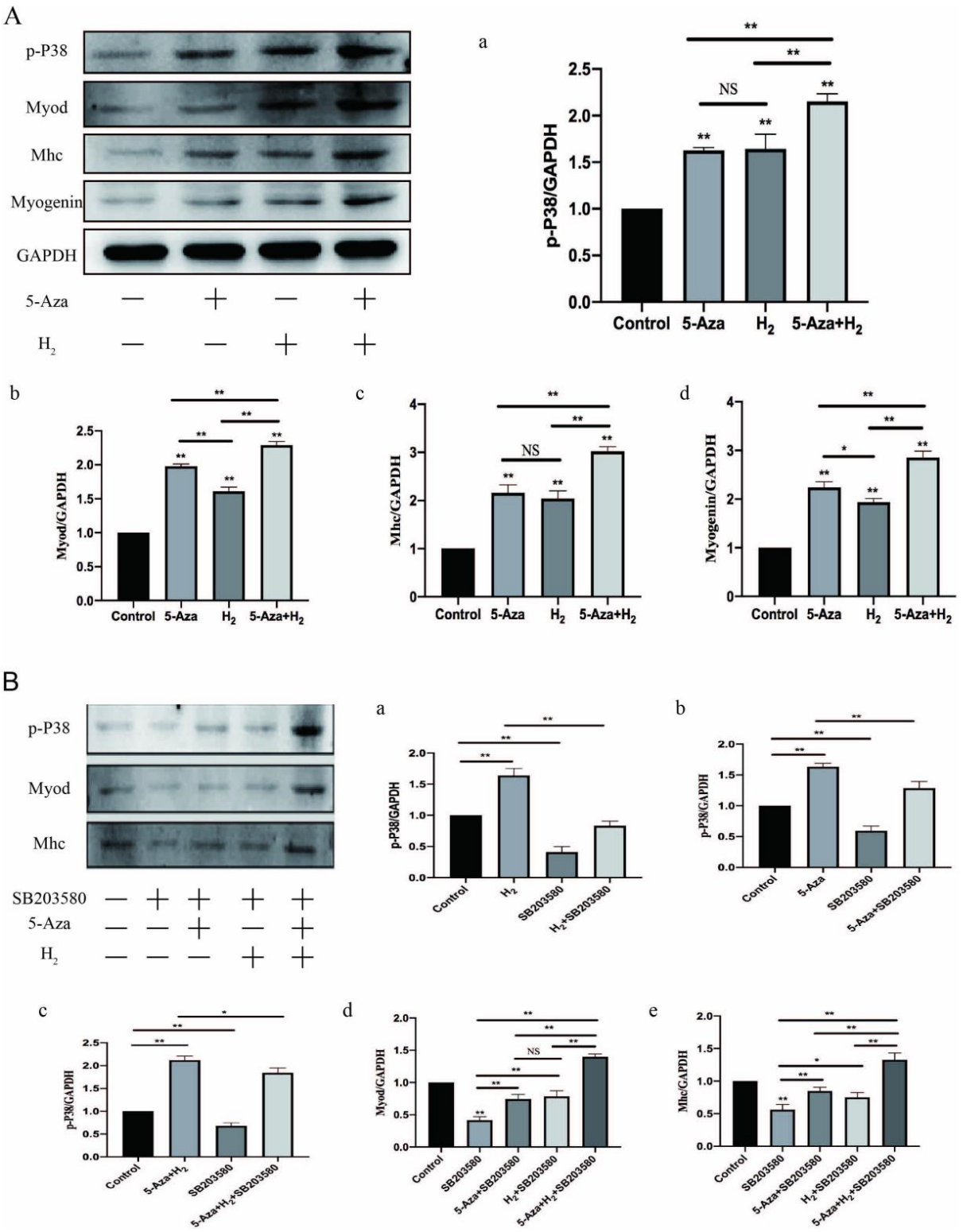

Fig. 4. (A) Myod, Mhc, Myogenin and p-P38 and expression (Western blot). (B) Molecular mechanism analysis of myogenic differentiation. (B) Western blot analysis of p38 MAPK pathway related proteins in ADSCs on day 7 after incubation with inductor in inhibitor added myogenic differentiation medium; Quantitative gray level based on the Western blot bands for p-P38, Mhc and Myod proteins expression; All experiments were performed in triplicate (*$p<0.05$, **$p<0.01$).

matics and literature reports, it is known that p38 MAPK was indicated to participate in a range of biological processes of myogenic differentiation. Accordingly, We assessed whether phosphorylation levels of p38 MAPK are influenced by H_2 combined with 5-Aza regulation during myogenic differentiation. ADSCs were incubated in DMEM for 7 days. According to Fig. 4A, the level of p-P38 in the 5-Aza and H_2 cotreatment group was significantly greater than that in the control ($p<0.01$), which indicated an enhancement in the active form of p38 that promotes differentiation. This result suggests that 5-Aza and H_2 cotreatment during myogenic differentiation could improve p38 activity. It is noteworthy that the levels of p-P38 in the 5-Aza and H_2 single-treatment groups also significantly increased compared with those in the control, which indicated that either 5-Aza or H_2 treatment during myogenic differentiation increases p38 activity.

Myogenic differentiation promoted by hydrogen in combination with 5-Aza is disrupted by pharmacological inhibition of p38

H_2 combined with 5-Aza improved p-P38 in ADSCs. The mentioned effect, however, was abolished by the presence of specific concentrations of SB203580 (5 nM), a pharmacological inhibitor of p38 that has been established and applied extensively. For a broader analysis of the variations in protein, the Western blotting assay was conducted on Myod and Mhc proteins after 7 days of incubation in DMEM with or without SB203580. In addition, the protein expression of Myod was significantly increased in the remaining three groups (5-Aza+SB203580, H_2+SB203580 and 5-Aza+H_2+SB203580) compared to the SB203580 group ($p<0.01$). The protein expression of Mhc was significantly increased in 5-Aza+SB203580 and 5-Aza+H_2+SB203580 groups compared to SB203580 group ($p<0.01$). The protein expression of Mhc was increased in H_2+SB203580 groups compared to SB203580 group ($p<0.05$). Compared to the rest of the experimental groups (5-Aza+SB203580 and H_2+SB203580), the 5-Aza +H_2+SB203580 group exhibited the highest protein expression of Myod and Mhc ($p<0.01$). Subsequently, the protein expression of signaling pathway during the myoblast differentiation was detected. The level of p-P38 was significantly decreased after the introduction of the inhibitor compared to the control group ($p<0.01$). Compared to the SB203580 group, p-P38 was significantly more highly expressed in the other three groups ($p<0.01$) (i.e. H_2+SB203580, 5-Aza+SB203580 and H_2+5-Aza+ SB203580). In addition, the following three groups (H_2, 5-Aza and H_2+5-Aza) showed significantly higher expression of P-p38 compared to the three groups after the addition of inhibitors respectively ($p<0.01$). For this reason, SB203580 prevents muscle fusion, whereas three group except for SB203580 could still promote myogenic differentiation. In brief, the combination of H_2 and 5-Aza can activate the p38 MAPK signalling pathway by increasing the levels of p-P38 protein to promote myogenic differentiation of ADSCs.

Discussion

The aim of this study was to investigate the role of H_2 combined with 5-Aza in promoting the proliferation and myogenic differentiation of ADSCs, and the signalling pathways that may be involved. H_2 has been proven to be used in multiple biological systems, including those in the Cardiovascular, Digestive and Motor System (28). In the present study, the H_2 and 5-Aza cotreatment can result from the following: 1) reinforcing the single-cell mitochondrial number; 2) stimulating the myogenic biomarking genes' expressing state pertaining to Mhc and Myod, etc.; 3) promoting p38 phosphorylating process inside MAP kinases (MAPK) signaling pathway, by leading the promoted myoblast differentiation.

Over the past few years, uses of H_2 have been largely anticipated as novel medical treatments (29). H_2 has been employed in different forms to various disease models, and research on its curative effects has progressed rapidly (16, 30). In the present study, H_2-induced ADSCs were confirmed to exhibit a high biocompatibility *in vitro* based on MTT and Live-Dead Cell Staining (Fig. 2). Notably, hydrogen both promotes the proliferation of ADSCs and reduces the cytotoxicity of 5-Aza, thereby improving cell viability. Accordingly, H_2 can be significantly ensured to promote the myogenic differentiation of ADSCs. Mitochondria, one of the vital intracellular organelles, significantly impacts various biological processes of eukaryotic cells (e.g., energy generation, calcium balance, intracellular substance metabolism, reactive oxygen production, cell signal transduction and apoptosis (31-33). As indicated from the recent advances, adequate mitochondrial function in stem cells is essential to maintain proliferation and differentiation abilities (34, 35). Accordingly, green mito-tracker staining was adopted to explain the effect of H_2 on the mitochondria of ADSCs. The fluorescence intensity of single cell mitochondria significantly increased after H_2 induction. For this reason, the promoted proliferation of ADSCs was probably because H_2 could increase the mitochondrial number.

Myod and Mhc, the early and late markers of myo-

genesis (36, 37), were used to determine the myogenic differentiation at mRNA, protein and myotube formation. In the present study, levels of Myod and Mhc both increased significantly when H_2 induction. Notably, H_2 and 5-Aza can synergistically promote the myogenic differentiation of ADSCs. In ADSCs was evaluated using desmin immunofluorescence. Desmin, a muscle-specific member of the family of intermediate filaments, is one of the earliest appearing myogenic markers in both skeletal and heart muscles (38). Our immunofluorescence results showed that Desmin was significantly overexpressed in H_2-induced ADSCs. Interestingly, in myotubule observation, H_2 and 5-Aza still promoted myotubule maturation under the continuous action of SB203580 (Fig. 3B). Therefore, this result indicates that the first is that 5-Aza and H_2 can compete with the p38 MAPK signaling pathway to promote myobgenic differentiation. The second is that H_2 promotes myogenic differentiation via the p38 MAPK signaling pathway, but not only via the p38 MAPK signaling pathway (Fig. 3B). It has been reported that the myogenic differentiation and myoblast's myotube formation noticeably relied upon cell proliferation (Singh and Dilworth 2013) (39). The balance between myoblast proliferation and differentiation is important during muscle development (40). In the present study, the results of the above cell proliferation and myogenic differentiation show a certain correlation. The process of myogenic differentiation into myotube formation is often accompanied by changes in mitochondrial energy metabolism and ROS production. Previous studies have shown that Reactive oxygen species (ROS) is essential mediators of muscle differentiation (41), and it has long been associated with skeletal muscle physiology (42, 43). However, with the accumulation of ROS, due to its strong oxidation, it can cause irreversible damage to proteins, nucleic acids, sugars, lipids, etc., which significantly inhibits cell activity and leads to cell apoptosis (44, 45). In the process of myogenic differentiation of stem cells, intracellular ROS level is significantly increased, and the expression of apoptotic proteins such as p53 and other genes is also significantly increased, and cell activity is significantly inhibited (46, 47).

Previous studies have shown that H_2 can reduce ROS level in radiation-injured mice, reduce liver damage, and inhibit radiation-induced apoptosis, thus proving that H_2 can play a protective role on radiation-induced immune system injury by eliminating ROS (48). The observation that H_2 treatment significantly improved the level of SH-SY5Y ATP and $\Delta\psi$m in neuroblastoma (49) is an indication that H_2 treatment can elevate energy metabolism in mitochondria by activating oxidative phosphorylation. In conclusion, H_2 can promote mitochondrial oxidative phosphorylation and maintain ROS dynamic balance to effectively protect the cell damage in the differentiation stage, and further promote the myogenic differentiation of stem cells. However, how mitochondrial function changes in the process of H_2-induced myogenic differentiation of stem cells remains to be studied.

As revealed from the mentioned results, H_2 could remarkably enhance ADSCs proliferation and myogenic differentiation, whereas the molecular system was unclear. Here, based on the p38 MAPK classes refer to signal transducing elements promoting myogenic differentiation *in vitro* and influencing muscle growing and repairing *in vivo*, whereas only p38 MAPK has a direct effect on myogenic transcribing elements of the Myod class (50, 51). And through bioinformatics analysis infer H_2 was speculated to be involved in the p38 MAPK signaling pathway, probably affecting myogenic differentiation. During the differentiation, skeletal muscle cell can proliferate, migrate, subsequently seed from the cell cycle associated with an improvement in p38 MAPK signaling activity and then fuse to form multinucleated myotubes (52, 53). To verify whether H_2 combined with 5-Aza-induced myogenic differentiation requires the effect of p38 signaling activity, a p38 MAPK kinase inhibitor (SB203580) capable of blocking p38 phosphorylation was used in this study. The results of Western blotting assay showed that co-treatment of H_2 and 5-Aza could enhance the phosphorylation process of p38 and thus improve myogenic differentiation. When inhibitors (SB203580) were added, p-P38 expressions were significantly reduced. The results indicate that co-treatment of H_2 and 5-Aza stimulates the p38 MAPK signaling pathway to promote myogenic differentiation.

Notably, the 5-Aza+H_2 group still had a synergistic effect to promote myogenic differentiation of ADSCs. The synergistic effect may be explained by the fact: Firstly, H_2 can enhance cell viability by attenuating the cytotoxicity of 5-Aza. Myogenic differentiation and myotube formation in myogenic cells have been reported to be significantly dependent on cell proliferation. Thus, this resulted in a higher myogenic differentiation effect. Secondly, we demonstrated by overexpression of p-P38 protein that the 5-Aza+H_2 group could promote myogenic differentiation of ADSCs through the p38 MAPK signalling pathway.

However, this study is limited as only *in vitro* experiments were performed. Future studies should therefore perform *in vivo* experiments to confirm these results.

In conclusions, in brief, this study suggested that H_2 can promote myogenic differentiation via the p38 MAPK sig-

naling pathways. H_2 also has a synergistic effect with 5-Aza to promote adipose stem cell proliferation and myogenic differentiation. Thus, the mentioned results are likely to elucidate myogenic differentiation and provide a high safety and efficacy alternative strategy for muscle damage and degeneration.

Ethics approval and consent to participate

All animal experiments were performed under the approval of the Institutional Animal Care and Use Committee of Jiangsu University.

Acknowledgments

This work was supported by the funds from the young medical key talent project of Jiangsu province (contract number QNRC2016458). Jiangsu Provincial Medical Innovation Team (Grant#CXTDB2017004).

Potential Conflict of Interest

The authors have no conflicting financial interest.

Author Contributions

Wenyong Fei, Erkai Pang and Jingcheng Wang: conception and design, financial support, experiment, manuscript writing, final approval of manuscript.

Erkai Pang made the equal contribution to the article and should be considered co-first author. Correspondence: Jingcheng Wang.

Lei Hou, Jihang Dai, Mingsheng Liu, Xuanqi Wang, Bin Xie: analysis and interpretation of data and drafted the manuscript.

All authors read and approved the final manuscript.

References

1. Abmayr SM, Pavlath GK. Myoblast fusion: lessons from flies and mice. Development 2012;139:641-656
2. Greising SM, Warren GL, Southern WM, Nichenko AS, Qualls AE, Corona BT, Call JA. Early rehabilitation for volumetric muscle loss injury augments endogenous regenerative aspects of muscle strength and oxidative capacity. BMC Musculoskelet Disord 2018;19:173
3. Aguilar CA, Greising SM, Watts A, Goldman SM, Peragallo C, Zook C, Larouche J, Corona BT. Multiscale analysis of a regenerative therapy for treatment of volumetric muscle loss injury. Cell Death Discov 2018;4:33 Erratum in: Cell Death Discov 2018;5:16
4. Valencia Mora M, Ruiz Ibán MA, Díaz Heredia J, Barco Laakso R, Cuéllar R, García Arranz M. Stem cell therapy in the management of shoulder rotator cuff disorders. World J Stem Cells 2015;7:691-699
5. Hernigou P, Flouzat Lachaniette CH, Delambre J, Zilber S, Duffiet P, Chevallier N, Rouard H. Biologic augmentation of rotator cuff repair with mesenchymal stem cells during arthroscopy improves healing and prevents further tears: a case-controlled study. Int Orthop 2014;38:1811-1818
6. Gimble JM, Katz AJ, Bunnell BA. Adipose-derived stem cells for regenerative medicine. Circ Res 2007;100:1249-1260
7. Grottkau BE, Lin Y. Osteogenesis of adipose-derived stem cells. Bone Res 2013;1:133-145
8. Dai R, Wang Z, Samanipour R, Koo KI, Kim K. Adipose-derived stem cells for tissue engineering and regenerative medicine applications. Stem Cells Int 2016;2016:6737345
9. Xie X, Wang Y, Zhao C, Guo S, Liu S, Jia W, Tuan RS, Zhang C. Comparative evaluation of MSCs from bone marrow and adipose tissue seeded in PRP-derived scaffold for cartilage regeneration. Biomaterials 2012;33:7008-7018
10. Liu Y, Yan X, Sun Z, Chen B, Han Q, Li J, Zhao RC. Flk-1+ adipose-derived mesenchymal stem cells differentiate into skeletal muscle satellite cells and ameliorate muscular dystrophy in mdx mice. Stem Cells Dev 2007;16:695-706
11. Abdanipour A, Tiraihi T, Delshad A. Trans-differentiation of the adipose tissue-derived stem cells into neuron-like cells expressing neurotrophins by selegiline. Iran Biomed J 2011;15:113-121
12. Mizuno H, Zuk PA, Zhu M, Lorenz HP, Benhaim P, Hedrick MH. Myogenic differentiation by human processed lipoaspirate cells. Plast Reconstr Surg 2002;109:199-209; discussion 210-211
13. McClure MJ, Garg K, Simpson DG, Ryan JJ, Sell SA, Bowlin GL, Ericksen JJ. The influence of platelet-rich plasma on myogenic differentiation. J Tissue Eng Regen Med 2016;10:E239-E249
14. Zhao P, Jin Z, Chen Q, Yang T, Chen D, Meng J, Lu X, Gu Z, He Q. Local generation of hydrogen for enhanced photothermal therapy. Nat Commun 2018;9:4241
15. Ohsawa I, Ishikawa M, Takahashi K, Watanabe M, Nishimaki K, Yamagata K, Katsura K, Katayama Y, Asoh S, Ohta S. Hydrogen acts as a therapeutic antioxidant by selectively reducing cytotoxic oxygen radicals. Nat Med 2007;13:688-694
16. Ono H, Nishijima Y, Adachi N, Sakamoto M, Kudo Y, Nakazawa J, Kaneko K, Nakao A. Hydrogen(H2) treatment for acute erythymatous skin diseases. A report of 4 patients with safety data and a non-controlled feasibility study with H2 concentration measurement on two volunteers. Med Gas Res 2012;2:14
17. Guan P, Sun ZM, Luo LF, Zhou J, Yang S, Zhao YS, Yu FY, An JR, Wang N, Ji ES. Hydrogen protects against chronic intermittent hypoxia induced renal dysfunction by promoting autophagy and alleviating apoptosis. Life Sci 2019;225:46-54
18. Li J, Hong Z, Liu H, Zhou J, Cui L, Yuan S, Chu X, Yu P. Hydrogen-rich saline promotes the recovery of renal function after ischemia/reperfusion injury in rats via an-

ti-apoptosis and anti-inflammation. Front Pharmacol 2016; 7:106
19. Miyazaki N, Yamaguchi O, Nomiya M, Aikawa K, Kimura J. Preventive effect of hydrogen water on the development of detrusor overactivity in a rat model of bladder outlet obstruction. J Urol 2016;195:780-787
20. Quan-Jun Y, Yan H, Yong-Long H, Li-Li W, Jie L, Jin-Lu H, Jin L, Peng-Guo C, Run G, Cheng G. Selumetinib attenuates skeletal muscle wasting in murine cachexia model through ERK inhibition and AKT activation. Mol Cancer Ther 2017;16:334-343
21. Suzuki A, Minamide R, Iwata J. WNT/β-catenin signaling plays a crucial role in myoblast fusion through regulation of nephrin expression during development. Development 2018;145:dev168351
22. Low S, Barnes JL, Zammit PS, Beauchamp JR. Delta-like 4 activates Notch 3 to regulate self-renewal in skeletal muscle stem cells. Stem Cells 2018;36:458-466
23. Böhm A, Hoffmann C, Irmler M, Schneeweiss P, Schnauder G, Sailer C, Schmid V, Hudemann J, Machann J, Schick F, Beckers J, Hrabě de Angelis M, Staiger H, Fritsche A, Stefan N, Nieß AM, Häring HU, Weigert C. TGF-β contributes to impaired exercise response by suppression of mitochondrial key regulators in skeletal muscle. Diabetes 2016;65:2849-2861
24. Yi C, Liu D, Fong CC, Zhang J, Yang M. Gold nanoparticles promote osteogenic differentiation of mesenchymal stem cells through p38 MAPK pathway. ACS Nano 2010;4:6439-6448
25. Lassar AB. The p38 MAPK family, a pushmi-pullyu of skeletal muscle differentiation. J Cell Biol 2009;187:941-943
26. Jones NC, Tyner KJ, Nibarger L, Stanley HM, Cornelison DD, Fedorov YV, Olwin BB. The p38alpha/beta MAPK functions as a molecular switch to activate the quiescent satellite cell. J Cell Biol 2005;169:105-116
27. Wakitani S, Saito T, Caplan AI. Myogenic cells derived from rat bone marrow mesenchymal stem cells exposed to 5-azacytidine. Muscle Nerve 1995;18:1417-1426
28. Yang M, Dong Y, He Q, Zhu P, Zhuang Q, Shen J, Zhang X, Zhao M. Hydrogen: a novel option in human disease treatment. Oxid Med Cell Longev 2020;2020:8384742
29. Ohta S. Molecular hydrogen as a preventive and therapeutic medical gas: initiation, development and potential of hydrogen medicine. Pharmacol Ther 2014;144:1-11
30. Huang CS, Kawamura T, Toyoda Y, Nakao A. Recent advances in hydrogen research as a therapeutic medical gas. Free Radic Res 2010;44:971-982
31. Smith GCS, Bouwmeester TM, Lam PH. Knotless double-row SutureBridge rotator cuff repairs have improved self-reinforcement compared with double-row SutureBridge repairs with tied medial knots: a biomechanical study using an ovine model. J Shoulder Elbow Surg 2017;26:2206-2212
32. Kim KC, Shin HD, Cha SM, Park JY. Comparisons of re-tear patterns for 3 arthroscopic rotator cuff repair methods. Am J Sports Med 2014;42:558-565
33. Killian ML, Cavinatto LM, Ward SR, Havlioglu N, Thomopoulos S, Galatz LM. Chronic degeneration leads to poor healing of repaired massive rotator cuff tears in rats. Am J Sports Med 2015;43:2401-2410
34. Papa L, Djedaini M, Hoffman R. Mitochondrial role in stemness and differentiation of hematopoietic stem cells. Stem Cells Int 2019;2019:4067162
35. Zhang H, Menzies KJ, Auwerx J. The role of mitochondria in stem cell fate and aging. Development 2018;145:dev143420
36. Ciciliot S, Schiaffino S. Regeneration of mammalian skeletal muscle. Basic mechanisms and clinical implications. Curr Pharm Des 2010;16:906-914 Erratum in: Curr Pharm Des 2015;21:4657
37. Yu X, Zhang Y, Li T, Ma Z, Jia H, Chen Q, Zhao Y, Zhai L, Zhong R, Li C, Zou X, Meng J, Chen AK, Puri PL, Chen M, Zhu D. Long non-coding RNA Linc-RAM enhances myogenic differentiation by interacting with MyoD. Nat Commun 2017;8:14016
38. Paulin D, Li Z. Desmin: a major intermediate filament protein essential for the structural integrity and function of muscle. Exp Cell Res 2004;301:1-7
39. Singh K, Dilworth FJ. Differential modulation of cell cycle progression distinguishes members of the myogenic regulatory factor family of transcription factors. FEBS J 2013;280:3991-4003
40. Yokoyama S, Asahara H. The myogenic transcriptional network. Cell Mol Life Sci 2011;68:1843-1849
41. Le Moal E, Pialoux V, Juban G, Groussard C, Zouhal H, Chazaud B, Mounier R. Redox control of skeletal muscle regeneration. Antioxid Redox Signal 2017;27:276-310
42. Ji LL, Kang C, Zhang Y. Exercise-induced hormesis and skeletal muscle health. Free Radic Biol Med 2016;98:113-122
43. Mason SA, Morrison D, McConell GK, Wadley GD. Muscle redox signalling pathways in exercise. Role of antioxidants. Free Radic Biol Med 2016;98:29-45
44. Gibbons MC, Singh A, Engler AJ, Ward SR. The role of mechanobiology in progression of rotator cuff muscle atrophy and degeneration. J Orthop Res 2018;36:546-556
45. Oh JH, Chung SW, Kim SH, Chung JY, Kim JY. 2013 neer award: effect of the adipose-derived stem cell for the improvement of fatty degeneration and rotator cuff healing in rabbit model. J Shoulder Elbow Surg 2014;23:445-455
46. Pas HIMFL, Moen MH, Haisma HJ, Winters M. No evidence for the use of stem cell therapy for tendon disorders: a systematic review. Br J Sports Med 2017;51:996-1002
47. Osborne H, Anderson L, Burt P, Young M, Gerrard D. Australasian College of Sports Physicians-position statement: the place of mesenchymal stem/stromal cell therapies in sport and exercise medicine. Br J Sports Med 2016; 50:1237-1244
48. Saito T, Sadoshima J. Molecular mechanisms of mitochondrial autophagy/mitophagy in the heart. Circ Res 2015; 116:1477-1490
49. Murakami Y, Ito M, Ohsawa I. Molecular hydrogen protects against oxidative stress-induced SH-SY5Y neuroblastoma cell death through the process of mitohormesis.

PLoS One 2017;12:e0176992
50. Qi R, Liu H, Wang Q, Wang J, Yang F, Long D, Huang J. Expressions and regulatory effects of P38/ERK/JNK Mapks in the adipogenic trans-differentiation of C2C12 myoblasts. Cell Physiol Biochem 2017;44:2467-2475
51. Bernet JD, Doles JD, Hall JK, Kelly Tanaka K, Carter TA, Olwin BB. p38 MAPK signaling underlies a cell-autonomous loss of stem cell self-renewal in skeletal muscle of aged mice. Nat Med 2014;20:265-271
52. Brien P, Pugazhendhi D, Woodhouse S, Oxley D, Pell JM. p38α MAPK regulates adult muscle stem cell fate by restricting progenitor proliferation during postnatal growth and repair. Stem Cells 2013;31:1597-1610
53. Cuenda A, Sanz-Ezquerro JJ. p38γ and p38δ: from spectators to key physiological players. Trends Biochem Sci 2017;42:431-442